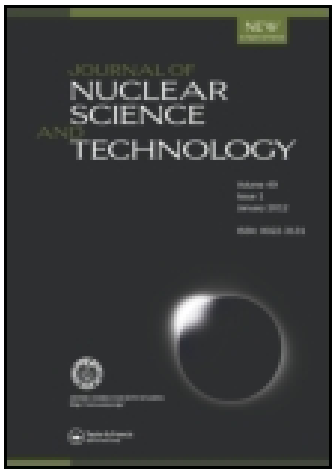

Journal of Nuclear Science and Technology
Publication details, including instructions for authors and subscription information:
http://www.tandfonline.com/loi/tnst20

Study on Effective Average (γ, n) Cross Section for ^{89}Y, ^{90}Zr, ^{93}Nb, and ^{133}Cs and (γ, 3n) Cross Section for ^{99}Tc

Abul Kalam Md. Lutfor RAHMAN [a] , Kunio KATO [a] , Hidehiko ARIMA [a] , Nobuhiro SHIGYO [a] , Kenji ISHIBASHI [a] , Jun-ichi HORI [b] & Ken NAKAJIMA [b]

[a] Department of Applied Quantum Physics and Nuclear Engineering , Kyushu University , 744 Motooka, Nishi-ku, Fukuoka , 819-0395 , Japan

[b] Kyoto University Research Reactor Institute , Osaka , 590-0494 , Japan

Published online: 05 Jan 2012.

To cite this article: Abul Kalam Md. Lutfor RAHMAN , Kunio KATO , Hidehiko ARIMA , Nobuhiro SHIGYO , Kenji ISHIBASHI , Jun-ichi HORI & Ken NAKAJIMA (2010) Study on Effective Average (γ, n) Cross Section for ^{89}Y, ^{90}Zr, ^{93}Nb, and ^{133}Cs and (γ, 3n) Cross Section for ^{99}Tc, Journal of Nuclear Science and Technology, 47:7, 618-625, DOI: 10.1080/18811248.2010.9720959

To link to this article: http://dx.doi.org/10.1080/18811248.2010.9720959

Journal of NUCLEAR SCIENCE and TECHNOLOGY, Vol. 47, No. 7, p. 618–625 (2010)

ARTICLE

Study on Effective Average (γ, n) Cross Section for ^{89}Y, ^{90}Zr, ^{93}Nb, and ^{133}Cs and (γ, 3n) Cross Section for ^{99}Tc

Abul Kalam Md. Lutfor RAHMAN[1,*,†], Kunio KATO[1], Hidehiko ARIMA[1], Nobuhiro SHIGYO[1], Kenji ISHIBASHI[1], Jun-ichi HORI[2] and Ken NAKAJIMA[2]

[1]*Department of Applied Quantum Physics and Nuclear Engineering, Kyushu University, 744 Motooka, Nishi-ku, Fukuoka 819-0395, Japan*
[2]*Kyoto University Research Reactor Institute, Osaka 590-0494, Japan*

(Received June 3, 2009 and accepted in revised form March 1, 2010)

A nondestructive detection technique was proposed for the easy assessment of long-lived radionuclides by the use of bremsstrahlung photons. The nuclide of ^{99}Tc was considered for the assessment over an effective average ^{99}Tc (γ, 3n) ^{96}Tc cross section. For validating the experimental method on ^{99}Tc, photonuclear (γ, n) cross sections of ^{89}Y, ^{90}Zr, ^{93}Nb, and ^{133}Cs were measured. Continuous-energy bremsstralung photons were generated from a platinum target bombarded by an electron beam of 32/36 MeV from an electron linac. The photonuclear (γ, n) cross sections were previously measured by Saclay (France) and Livermore (USA) laboratories for ^{89}Y, ^{90}Zr, ^{93}Nb, and ^{133}Cs nuclides. For ^{89}Y, ^{90}Zr, and ^{133}Cs, the present results were in good agreement, within 9% deviation with Saclay and an acceptable deviation of 14–36% from Livermore. In the case of ^{93}Nb, the contribution for ^{93}Nb (γ, n) ^{92}Nb* in the metastable state was 55.2% of the total (γ, n) cross section of Saclay in an averaged form. The present experimental method was thus confirmed to show a good accuracy. The effective average cross section of ^{99}Tc (γ, 3n) ^{96}Tc was obtained as 2.30 mb in the energy range of 25.723–36 MeV.

KEYWORDS: bremsstrahlung photons, photonuclear reaction, nondestructive detection, easy assessment, long-life radionuclei, effective average cross section, electron linac, waste drum, radioactivity, HPGe detector

I. Introduction

Many radioactive waste nuclides are produced from nuclear facilities. Among them, ^{129}I and ^{99}Tc have half-lives of millions of years and account for a significant presence in nuclear waste. A nondestructive detection technique is proposed for easier assessment of the long-lived nuclides through photonuclear reaction measurement. High-energy bremsstralung photons generated by an electron linear accelerator are focused directly into the waste drum. Long-lived non-gamma-emitting nuclides are converted into short-lived gamma emitters through photon-induced reaction. Our group already has successfully measured the effective average ^{129}I (γ, n) ^{128}I cross section using this nondestructive detection technique.[1)]

The nuclide of ^{99}Tc is a great concern because of its significant existence in long-lived fission waste and its potential health risk. It is generally soluble in water under geologic conditions and may migrate relatively quickly in common ground water, eventually entering the food chain. Therefore, before geologic disposal, it is necessary to determine the amount present in nuclear waste. If long-lived β-radionuclides such as ^{99}Tc (half-life of 2.11×10^5 years) can be converted into the short-lived gamma emitter ^{96}Tc (half-life of 4.28 days) through the photonuclear reaction of ^{99}Tc (γ, 3n) ^{96}Tc, its radioactivity can easily be measured by counting gamma rays from the outside of the drum. The photonuclear cross section of ^{99}Tc (γ, 3n) ^{96}Tc is required for the nondestructive detection technique, but has not been measured so far. The objective of this study is to measure the photonuclear cross section of ^{99}Tc (γ, 3n) ^{96}Tc. Before the experiment was performed on ^{99}Tc, the photonuclear reaction cross sections were measured for some naturally existing nuclides to validate the present experimental method. The following reactions were chosen: ^{89}Y (γ, n) ^{88}Y, ^{90}Zr (γ, n) ^{89}Zr, ^{93}Nb (γ, n) ^{92}Nb, and ^{133}Cs (γ, n) ^{132}Cs.

Extensive measurements of photon-induced reaction cross sections have been performed at different laboratories covering the Giant Dipole Resonance (GDR) energy region, but there are still considerable discrepancies in both shapes and magnitudes between the obtained data, not only in experi-

*Corresponding author, E-mail: rahman@cstf.kyushu-u.ac.jp
†Present address: *Dept. of Applied Chemistry, Kyushu University, 744 Motooka, Nishi-ku, Fukuoka 819-0395, Japan*

ments of different types but in experiments of the same type as well.[2–4] Therefore, precision in the photonuclear cross section data is in high demand for engineering applications.

In this research, the effective average (γ, n) cross section for the stable nuclides of ^{89}Y, ^{90}Zr, ^{93}Nb, and ^{133}Cs, and (γ, 3n) cross section for the long-lived nuclide of ^{99}Tc were measured by using bremsstrahlung photons produced from a linac bombarded by 32 and 36 MeV incident electron energies, respectively.

II. Experiment

The irradiation experiment was carried out by using the electron linear accelerator (linac) at the Kyoto University Research Reactor Institute. The electron beam center was roughly found by performing a short irradiation and placing a plastic monitor film in front of the bremsstrahlung target. The electron beam distribution around the sample was also monitored using a second plastic film.

Thin gold tapes were placed in horizontal and vertical directions across the approximate center of the electron beam spot in front of the sample position to produce the photon beam center. The thin tapes were irradiated for 5 min. After irradiation, the tapes were cut into several 5-mm-long pieces. Gamma rays from the residual nuclide of ^{197}Au (γ, n) ^{196}Au were measured using a high-purity germanium (HPGe) detector. Counts of the photon peak at 355.73 keV were obtained. **Figure 1** shows the photon peak counts from the irradiated gold tapes in the horizontal and vertical directions. The highest counts in both directions were taken as the center of the photon beam where the samples were to be placed for irradiation.

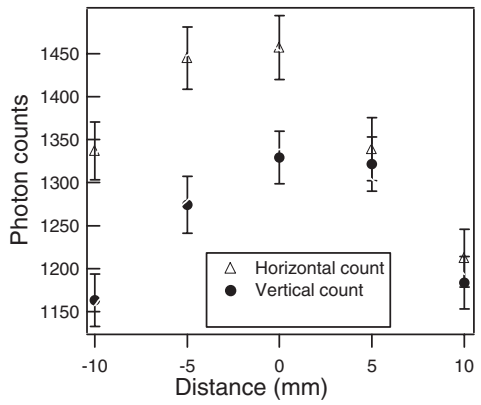

Fig. 1 Photon counts of the irradiated gold tapes in the horizontal and vertical directions

A platinum target was not thick enough for energetic electrons to be stopped within the target. Therefore a strong magnetic field was used to divert the passing electrons as shown in **Fig. 2**. The presence of the passing electrons on the sample area was checked by measuring the current in the sample holder and confirming that no current was found.

1. Irradiation for ^{89}Y (γ, n) ^{88}Y, ^{90}Zr (γ, n) ^{89}Zr, ^{93}Nb (γ, n) ^{92}Nb, and ^{133}Cs (γ, n) ^{132}Cs

Powder samples of Y_2O_3 and CsBr with weights of 0.03475 and 0.03517 g, respectively, were chosen for yttrium and cesium and they were formed into 9-mm-diameter pellets for irradiation. Zirconium (natural abundance of ^{90}Zr was 51.45%) and niobium were used as target materials in the form of 9-mm-diameter foil samples. The thicknesses of the zirconium and niobium samples were 0.05 and 0.0254 mm, respectively. All the samples were irradiated at 32 MeV incident electron energy. Gold foils of the same size (9 mm diameter, 50 μm thickness) were placed in front of all the target samples to measure the photon flux.

2. Irradiation for ^{99}Tc (γ, 3n) ^{96}Tc

A sealed radioisotope source of ^{99}Tc was utilized for the measurement of the photonuclear reaction cross section of ^{99}Tc (γ, 3n) ^{96}Tc. The sample was enclosed in a 0.4-mm-thick aluminum case. The activity of the source sample was 37 MBq with an error of 5.4% at the reference date of 5 November 1999. It was in the form of TcO_2 and its weight was 72.5 mg. The source was fabricated by AEA Technology, Oxfordshire, England. The sample was irradiated together with gold foils placed in the front and back to measure the photon fluxes. The gold foils were of the same size as the active diameter of the ^{99}Tc sample.

Bremsstrahlung photons were generated by the platinum target that was placed near the extraction port of the accelerator. The geometrical positions of the target and sample are presented in Fig. 2. Four platinum plates each with dimensions of 20 mm length, 20 mm width, and 0.5 mm thickness were enclosed in a 2-mm-thick aluminum case. Coolant water flowed inside the target case. The irradiation conditions for all the target samples are listed in **Table 1**.

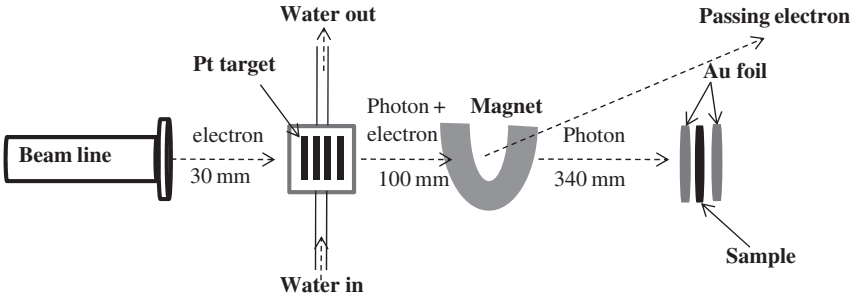

Fig. 2 Geometrical positions of materials and sample

Table 1 Irradiation conditions in the experiments

Target sample	Electron energy (MeV)	Irradiation time (s)	Average beam current (μA)	Bremsstrahlung target
^{89}Y and ^{133}Cs	32	1390	13.10	Pt
^{90}Zr	32	3660	13.08	
^{93}Nb	32	900	37	
^{99}Tc	36	3600	24.8	

Gamma rays from the decay of residual nuclides of irradiated samples and gold foils were measured using the HPGe detector. Detection efficiencies of the detector at different sample positions were calibrated by using standard sources. Counting of the samples and the gold foils was performed with the same geometry as the standard sources.

Decay data for the residual nuclides of ^{88}Y, ^{132}Cs, and ^{89}Zr are given in the literature[5–7] and they were taken into consideration for the data processing. From the decay scheme, it was seen that niobium has two energy states before beta decay. Since the ground state has a very long half-life of 3.5×10^7 years, it is impossible to measure the subsequent gamma emission. The excited state at 135.5 keV has a shorter half-life of 10.15 days and is easy to measure due to a sufficient rate of gamma decay from the product nuclide. After irradiation, the ^{99}Tc sample was left for 8 h for radioactivity cooling. The distance between the samples to the end cup surface of the detector was kept to an optimum to ensure a dead time counting of 1%. Measurements were made for several times in the case of the ^{99}Tc sample to observe the decay trend and check the half-life of the residual nuclide.

III. Data Analysis

1. Data Analysis on Gold Irradiation

Gold foils were irradiated together with the samples to determine the photon fluxes at the sample position. The photonuclear reaction on gold is ^{197}Au (γ, n) ^{196}Au. **Figure 3** shows an example of a gamma ray spectrum from the decay of the residual nuclide of the irradiated gold in front of the sample. The incident electron energy for the irradiation was 32 MeV with full width at half maximum (FWHM) of 2.8 MeV.

The peaks are at 355.73 keV ($I\gamma = 87\%$) for ^{196}Au decaying from the ^{197}Au (γ, n) ^{196}Au reaction and at 411.80 keV ($I\gamma = 95.6\%$) for ^{198}Au from the low-energy neutron-incident ^{197}Au (n, γ) ^{198}Au reaction. Use of the measured count rates, detection efficiency, decay time, branching ratios, and other data leads to activity A_0 at the end of irradiation by

$$A_0 = \frac{D}{\exp(-\lambda t_d)}\left(\frac{\lambda t_c}{1-\exp(-\lambda t_c)}\right), \quad (1)$$

where D: disintegrations per second as $C/\varepsilon P$,
C: net counting area of the photopeak/counting time,
ε: detection efficiency of the germanium detector,

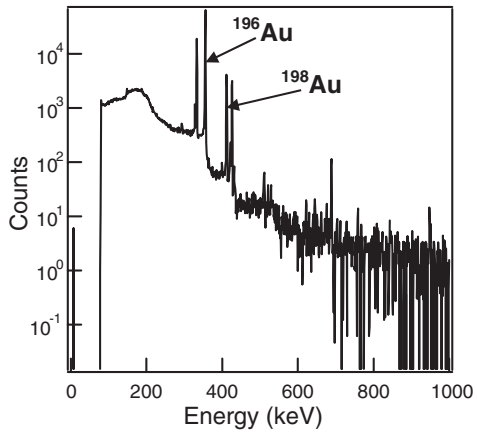

Fig. 3 Example of gamma spectrum from the residual nuclide of irradiated ^{197}Au foil in front of sample

P: branching ratio of the analyzed gamma ray,
λ: decay constant,
t_d: time duration for cooling, and
t_c: time duration for counting.

Activation yield A was derived from the activity A_0 as

$$A = N\int_{E_{th.}}^{E_{inc.}} \sigma\phi\, dE = \frac{A_0}{1-\exp(-\lambda t)}, \quad (2)$$

where N: number of target nuclei,
σ: cross section,
ϕ: photon flux,
t: irradiation time, and
$E_{th.}$ and $E_{inc.}$ are the threshold and incident energies, respectively.

Measured activation yields for the ^{197}Au (γ, n) ^{196}Au reaction were obtained at the front and back positions for different samples. Photon fluxes at the center of the samples were obtained by averaging the front and back gold activation data. The contribution of the secondary neutron reaction ^{197}Au (n, 2n) ^{196}Au was estimated. The value was found to be 0.02% of the ^{197}Au (γ, n) ^{196}Au reaction product and considered in data analysis.

2. Calculation of Photon Fluxes Using the EGS5 Code and Normalization by Gold Activation

The photon flux distribution was also calculated by using the EGS5 code with the same geometry used in the experiment. An example of the average flux distribution with respect to energy is presented in **Fig. 4**. The average was taken from photons incident on gold foils in the front and back of the sample at the nominal electron beam energy of 32 MeV.

The flux calculation for gold foil was made for each irradiation condition. There may be errors in the beam current measurement and in the experimental position alignment. The calculated fluxes were then normalized by the measured value of gold activation. The flux normalization factor f_N was obtained by using the following relation,

$$\frac{A'_{gold}}{A_{cal.}} = f_N, \quad (3)$$

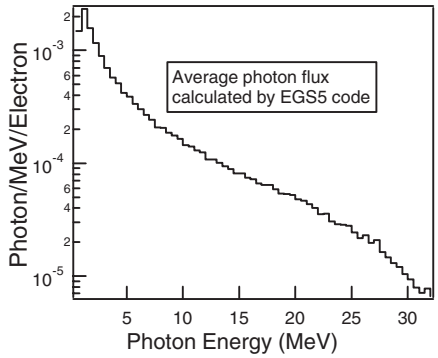

Fig. 4 Photon flux distribution calculated using the EGS5 code for electron beam energy of 32 MeV

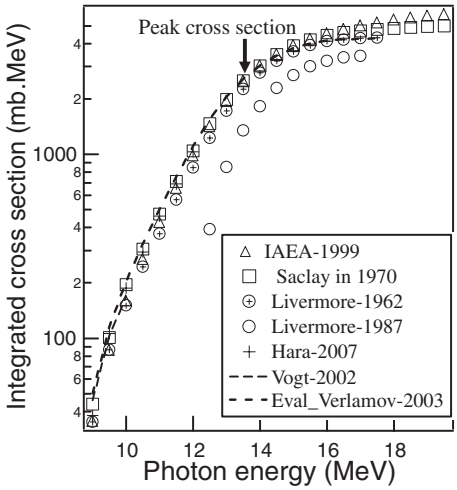

Fig. 5 Integrated cross section of ^{197}Au (γ, n) ^{196}Au reported by different groups. The energy at peak cross section is shown by an arrow.

where A'_{gold}: measured ^{197}Au (γ, n) ^{196}Au activation in our experiment,

$$A_{\text{cal.}} = \int_{E_{\text{th.}}}^{E_{\text{inc.}}} \sigma_{\text{other exp.}} \phi_{\text{cal.}} \mathrm{d}E, \tag{4}$$

$\sigma_{\text{other exp.}}$: ^{197}Au ($\gamma$, n) ^{196}Au cross section data from Saclay (France)[8] in the case of gold, and
$\phi_{\text{cal.}}$: flux calculated using the EGS5 code applying the same experimental condition.

Our data were compared with other experimental data published by Saclay or Livermore (USA). The exfor data from Saclay or Livermore are not available up to the incident energy range used in our experiment. Therefore, exfor data were extrapolated up to the incident energy. Extrapolation was made by factoring in the absorption cross section[13] over the (γ, 2n) energy region up to 19.8 MeV to meet the (γ, n) cross section trend. It was further extended up to the incident energy in our experiment by maintaining the same function. Photonuclear cross sections of ^{197}Au (γ, n) ^{196}Au have been reported by many groups[8–13] (**Fig. 5**). The Saclay cross section data were used for determining the normalization factor in this measurement. The justifications of taking Saclay data are discussed below.

From Fig. 5, it is seen that the evaluated cross sections from the KAERI data library[13] and Livermore in 1962[9] give a good agreement with the Saclay values[8] around the peak cross section region at 13.5 MeV. The experiments by Hara *et al.*[12] and Vogt *et al.*[11] superimpose the cross sections on the Saclay data. Cross sections evaluated by Varlamov *et al.*[10] also give a good agreement with Saclay over the photon energy range. For these reasons, it is supposed that the Saclay data are more reliable to use in the normalization.

The calculated flux was thus normalized by the relation stated below to reproduce the flux at the sample position:

$$\phi_{\text{nor.}} = f_N \phi_{\text{cal.}}, \tag{5}$$

where f_N is derived from the ratio between the measured and calculated activation. The normalized fluxes were used for the data analysis of the samples.

3. Data Analysis for the Effective Average Cross Section

The effective average cross sections from our measurement were obtained from

$$\sigma_{\text{meas.avg.}} = \frac{A'_{\text{sample}}}{N f_N \int_{E_{\text{th.}}}^{E_{\text{inc.}}} \phi_{\text{cal.}} \mathrm{d}E}, \tag{6}$$

where A'_{sample}: measured (γ, n) activation yield for the sample.

By using the normalized flux, the activations were calculated with the reported (Saclay, Livermore) cross section data for the nuclides other than gold using Eq. (4). The calculated effective average cross sections were determined as

$$\sigma_{\text{cal.avg.}} = \frac{f_N A_{\text{cal.}}}{\int_{E_{\text{th.}}}^{E_{\text{inc.}}} \phi_{\text{nor.}} \mathrm{d}E}, \tag{7}$$

where $A_{\text{cal.}}$ ($\int_{E_{\text{th.}}}^{E_{\text{inc.}}} \sigma_{\text{saclay/livermore}} \phi_{\text{cal.}} \mathrm{d}E$) is the calculated activation for a sample derived from the cross section reported by Saclay and Livermore, and $\phi_{\text{nor.}}$ is the normalized flux. Finally, the calculated average was compared with the measurement.

IV. Results and Discussion

1. Effective Average Cross Section for ^{89}Y (γ, n) ^{88}Y, ^{90}Zr (γ, n) ^{89}Zr, ^{93}Nb (γ, n) ^{92}Nb, and ^{133}Cs (γ, n) ^{132}Cs

Photonuclear cross sections of ^{89}Y (γ, n) ^{88}Y, ^{90}Zr (γ, n) ^{89}Zr, ^{93}Nb (γ, n) ^{92}Nb, and ^{133}Cs (γ, n) ^{132}Cs reactions were first measured in the Lawrence Livermore National Laboratory, Livermore, USA[14,15] and the C.E.N., Saclay, France.[16,17] The measurement technique adopted at both laboratories was a neutron counting method. Our data are based on gamma counting from the residual nuclide. Comparison was made between our data and those of Livermore and Saclay.

Activities of the samples at the end of irradiation and the average cross sections were obtained by using Eqs. (2) and (6). Photon flux energy distributions on gold foils were considered to obtain the flux in the sample position and calculated according to Sec. III-2.

Table 2 Effective average cross sections for ^{89}Y (γ, n) ^{88}Y, ^{90}Zr (γ, n) ^{89}Zr, ^{93}Nb (γ, n) ^{92}Nb, and ^{133}Cs (γ, n) ^{132}Cs

Nuclide	Result	Energy range considered (MeV)	Effective average cross section (barn)	Exp./Saclay	Exp./Livermore
^{89}Y	Our exp.	11.265–32	0.0776 (±0.0021)	1.03	1.36
	Saclay		0.0753 (±0.0028)		
	Livermore		0.0569 (±0.0021)		
^{90}Zr	Our exp.	11.971–32	0.0678 (±0.0031)	0.91	1.14
	Saclay		0.0745 (±0.0028)		
	Livermore		0.0596 (±0.0028)		
^{93}Nb	Our exp.	8.832–32	0.0299 (±0.0019)	(0.552)	
	Saclay		0.0542 (±0.0028)		
^{133}Cs	Our exp.	8.987–32	0.1032 (±0.0030)	1.02	1.25
	Saclay		0.1008 (±0.0024)		
	Livermore		0.0828 (±0.0059)		

Table 3 Principal sources of errors

Type of error (%)	^{89}Y (γ, n) ^{88}Y	^{90}Zr (γ, n) ^{89}Zr	^{93}Nb (γ, n) ^{92}Nb	^{133}Cs (γ, n) ^{132}Cs
Sample weight	0.2	0.2	0.22	0.03
Counting statistic	0.5	0.3	0.9	0.1
Efficiency calibration	1.8	3.3	4.0	2.1
Flux energy distribution	2.0	2.5	5.0	2
Total	2.7	4.2	6.5	2.9

*Uncertainty of γ-emission probability was given only for ^{89}Y (γ, n) ^{88}Y to be 0.3%. Since no data were given for other reactions, they were excluded in the consideration of total error.

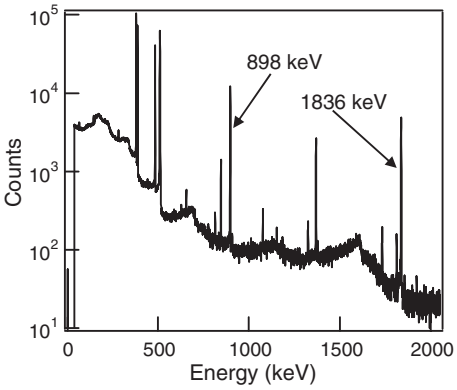

Fig. 6 Gamma ray spectrum from the decay product ^{88}Y

Figure 6 presents the experimental gamma ray spectrum from the β-decay product of ^{88}Y. Gamma rays are emitted at 898 and 1,836 keV with the absolute gamma intensities of 93.7 and 99%, respectively. The two peaks come into view in the figure. The average cross section data of ^{89}Y (γ, n) ^{88}Y, ^{90}Zr (γ, n) ^{89}Zr, ^{93}Nb (γ, n) ^{92}Nb, and ^{133}Cs (γ, n) ^{132}Cs reactions from our experiment and that of others (Saclay/Livermore) were obtained following the data analysis procedure described in Sec. III-3 and are summarized in **Table 2**. The contribution of ^{91}Zr (γ, 2n) ^{89}Zr was considered by taking into account the incident photon energy distribution and was found to be 9.00 ± 1.41% of the total experimental value from the residual nuclide of ^{89}Zr. Finally, the contribution of ^{91}Zr (γ, 2n) ^{89}Zr was subtracted from ^{90}Zr (γ, n) ^{89}Zr. Statistical and systematic errors were considered to determine the total error. All the sources of errors are given in **Table 3**.

It shows a good agreement between our result and the average cross section retrieved from the Saclay data. The values obtained from our measurements are 1.36, 1.14, and 1.25 times higher than the Livermore data in the case of ^{89}Y (γ, n) ^{88}Y, ^{90}Zr (γ, n) ^{89}Zr, and ^{133}Cs (γ, n) ^{132}Cs, respectively. The reason for such a deviation is attributed to the flux calculation applying the ^{197}Au (γ, n) ^{196}Au reaction performed by the Saclay group. If the flux calculation applied the ^{197}Au (γ, n) ^{196}Au reaction performed by the Livermore group, then this deviation would be reduced to a reasonable level. It was also reported[2] that the detection efficiency of the detector in the Livermore experiment was lower than that for Saclay. Therefore, the deviation between the Livermore results and our results can be ascribed to the same reason. It brings attention to the fact that our experimental method is applicable for the determination of photonuclear reaction cross sections in an easy way. These results help in the effort of performing the assessment of long-lived highly radioactive nuclides produced from nuclear waste.

The photonuclear ^{93}Nb (γ, n) ^{92}Nb reaction cross section covering the giant dipole region was measured only by the Saclay group[16] in 1971 using the neutron counting method. We made a comparison between that method and the gamma counting method.

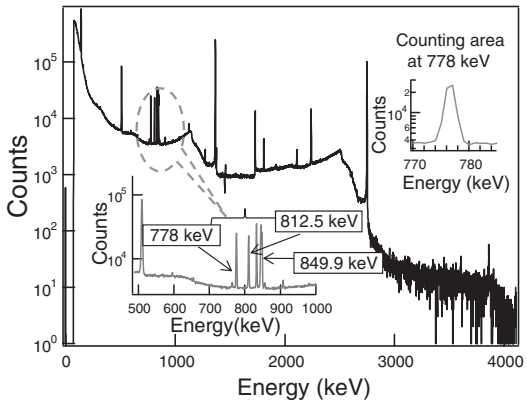

Fig. 7 Gamma ray spectrum from the beta decay product of ^{96}Tc

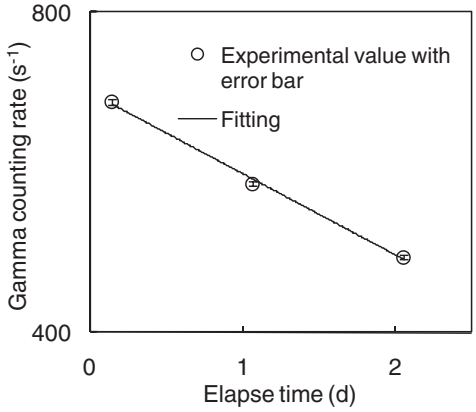

Fig. 8 Gamma ray counting rate at energy 778 keV *vs.* elapse time

The gamma ray emission from ^{92}Nb at 934.4 keV with an absolute gamma intensity of 99% represents the decay of ^{92}Zr, which is the β-decay product of ^{92}Nb. The effective average cross section obtained from our measurement deviates by 44.8% from the Saclay data. Measurement was performed by neutron counting in the Saclay laboratory. The product ^{92}Nb produces β-decays from the excited ($E_{\text{level}} = 135.5$ keV) and ground ($E_{\text{level}} = 0$ keV) states. Neutron counting data include both of these states. In the present study, however, gamma rays were measured from the β-decay of the (γ, n) product. Measurement of decaying gammas from the ground state of ^{92}Nb is impossible because of the quite long half-life ($T_{1/2} = 3.5 \times 10^7$ years). In our experimental result, gamma decays were considered only from the excited ($T_{1/2} = 10.15$ days) state. Thus, it concluded that the contribution of the excited state of ^{93}Nb (γ, n) ^{92}Nb* reaction was 55.2% of the total (γ, n) cross section of Saclay in an averaged form. A calculation was made from the decay data scheme,[18] taking the decay from the other energy state to the excited state into account. The calculation for the excited state gave a branching ratio of 59.7%, which supports the experimental result with a good agreement.

From the above consideration, we may come to the conclusion that our value is dependent on the photon-flux energy distribution, and the bremsstrahlung method is a feasible one to determine the relative value of photonuclear reaction cross sections.

2. Effective Average Cross Section for ^{99}Tc (γ, 3n) ^{96}Tc

Gamma ray spectrum from the beta product of ^{96}Tc produced from ^{99}Tc (γ, 3n) is presented in **Fig. 7**. In the spectrum, the peaks at 778 keV ($I\gamma = 99.76\%$), 812.5 keV ($I\gamma = 82\%$), and 849.9 keV ($I\gamma = 98\%$) are well observed and originated from the decay of ^{96}Mo, which is the β-decay product of ^{96}Tc. After irradiation, gamma rays were measured several times with the HPGe detector by taking the net peak area at 778 keV. The gamma ray counting rate *vs.* elapsed time is plotted in **Fig. 8**. The gamma counting rate decreases consistently with the half-life of ^{96}Tc of 4.28 days.

The activity at the end of irradiation and the activation yield were obtained by the method described in Sec. III. The effective average cross section at the energy range of 25.723 (threshold) to 36 (incident) MeV was obtained by using Eq. (8) and is listed in **Table 4**,

$$\sigma_{99_{\text{Tc}(\gamma,\,3n)}} = \frac{A'_{99_{\text{Tc}(\gamma,\,3n)}}}{f_N \int \phi_{\text{cal.}} \mathrm{d}E}, \tag{8}$$

where $A'_{99_{\text{Tc}(\gamma,\,3n)}}$ is the measured activation of ^{99}Tc (γ, 3n) ^{96}Tc reaction.

Table 4 Effective average cross section of ^{99}Tc (γ, 3n) ^{96}Tc reaction

Reaction	Energy range considered (MeV)	Effective average cross section at (mb)
^{99}Tc (γ, 3n) ^{96}Tc	25.723–36	2.30 ± 0.17

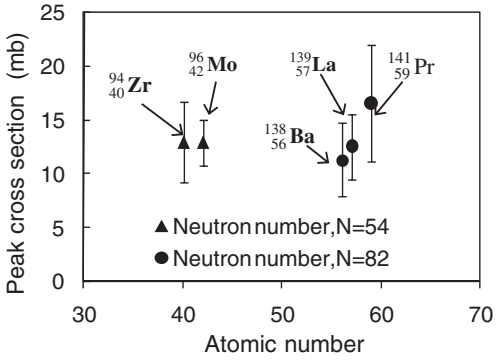

Fig. 9 (γ, 3n) cross sections of some vicinal nuclides with the same neutron number

Photonuclear (γ, 3n) cross sections gradually vary with changing atomic number Z and neutron number N of the nucleus. No large significant changes in cross sections were seen[19] between vicinal nuclei (especially elements with moderate mass number and the same neutron configuration). The reported (γ, 3n) cross sections of some vicinal nuclides with the same neutron number are shown in **Fig. 9**.[19] From the figure, no cross section deviation is seen among nuclei with the same neutron number of 54, that is, in the Mo and

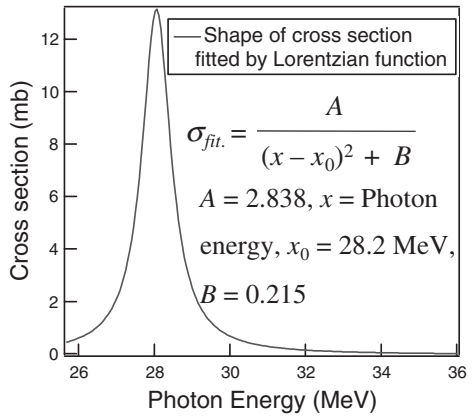

Fig. 10 Predicted shape of the cross section of ^{99}Tc (γ, 3n) ^{96}Tc reaction. The parameter "*A*" was treated to be adjustable.

Tc regions. In the case of the larger neutron number of 82, the cross sections are also almost comparable but tend to slightly increase with atomic number.

The element Mo is a close neighbor of Tc. Moreover, both ^{99}Tc and ^{98}Mo have the same neutron number condition. The existing cross section data of ^{98}Mo (γ, 3n) ^{95}Mo reaction were taken as the primary value and was extrapolated up to the incident energy in our measurement using a Lorentzian fitting function to meet our experimental effective average cross section value of 2.30 mb. Attention was also paid to the inclination of ^{98}Mo (γ, abs) cross sections in making the extrapolation. Considering the trends of changing cross sections mentioned in Fig. 9 and the cross section of ^{98}Mo (γ, 3n) ^{95}Mo[20] reaction, we attempted to obtain a predicted shape of the cross section of ^{99}Tc (γ, 3n) ^{96}Tc reaction. The predicted shape of the cross section of ^{99}Tc (γ, 3n) ^{96}Tc reaction is presented in **Fig. 10**. In the predicted fitting function, A is an adjustable parameter and X_0 and B are the constant parameters for the cross section trend of ^{98}Mo (γ, 3n) ^{95}Mo. The fitting function is also applicable to reproduce the (γ, 3n) cross sections of ^{94}Zr, ^{181}Ta, and ^{208}Pb nuclei within their error limits.

The cross section of ^{99}Tc (γ, 3n) ^{96}Tc reaction for different incident energies can be obtained using the above possible shape. Therefore, the effective average cross section measured in this experiment is a viable one to determine the amount of long-lived ^{99}Tc present in nuclear waste. The details of systematic and statistical errors are listed for ^{99}Tc (γ, 3n) ^{96}Tc in **Table 5**. The systematic error was assigned to be 5.4%, except the error of the reference cross section of ^{197}Au (γ, n) being 5.8%. The photon flux uncertainty in the target was included in the systematic error and was derived from the activation values of the front and back of the gold foils. The uncertainties in the flux energy distribution at the sample area and counting statistics were also considered in the table.

V. Conclusions

The photonuclear ^{99}Tc (γ, 3n) ^{96}Tc reaction is considered useful for assessing the quantity of the long-lived fission product nuclide ^{99}Tc. For validating the experimental method based on bremsstrahlung photons, the effective average photonuclear cross section measurements for some stable nuclei were measured. Photonuclear reactions of ^{89}Y (γ, n) ^{88}Y, ^{90}Zr (γ, n) ^{89}Zr, ^{93}Nb (γ, n) ^{92}Nb, and ^{133}Cs (γ, n) ^{132}Cs were chosen in the present study.

Our results agree well with the Saclay data within 9% deviation and an acceptable error of 14–36% with the Livermore data for ^{89}Y, ^{90}Zr, and ^{133}Cs nuclides. As our process only detected the gamma rays from the residual nuclide, it was easy to measure the reaction on the excited state of ^{92}Nb through the ^{93}Nb (γ, n) ^{92}Nb reaction. The influence obtained for the ^{93}Nb (γ, n) ^{92}Nb reaction in the excited state was 55.2% of the total (γ, n) cross section of Saclay in an averaged form. An approximate calculation of the branching ratio at the excited state was 59.7%, which supports the experimental result with a good agreement. Therefore, the results from the stable nuclide measurement confirmed the applicability of bremsstrahlung photons to the long-lived nuclide assessment.

We measured the effective average cross section for ^{99}Tc (γ, 3n) ^{96}Tc reaction and the value was 2.30 ($\pm$0.17) mb at the energy range of 25.723–36 MeV. The predicted cross section shape is usable to determine the cross section at different incident energies. The use of the measured average cross section of the ^{99}Tc (γ, 3n) ^{96}Tc reaction may provide reliability in the assessment of long-lived β-active radionuclides by the "nondestructive detection" technique.

Table 5 Systematic and statistical uncertainties for ^{99}Tc (γ, 3n) ^{96}Tc considered in the analysis

Uncertainty	Systematic (%)	Statistical (%)
Flux at the target position	0.1	
Flux energy distribution	2.0	
Efficiency calibration	5.0	
Counting statistics		0.7
Sample activity		5.4
Total	5.38	5.44
Total (systematic and statistical)%	7.65	

*Uncertainty of γ-emission probability for ^{99}Tc (γ, 3n) ^{96}Tc reaction was not reported in the decay data sheet; therefore, it was excluded in the total error.

Acknowledgement

We would like to express our gratitude to the staff of the Kyoto University Research Reactor Institute for providing us with the opportunity to use the linac and HPGe detector and for other support in successfully performing these experiments.

References

1) A. K. M. L. Rahman *et al.*, "Measurement of the photonuclear (γ, *n*) reaction cross section for ^{129}I using bremsstrahlung photons," *Nucl. Sci. Eng.*, **160**, 363–369 (2008).
2) B. L. Berman, S. C. Fultz, "Measurement of the giant dipole resonance with monoenergetic photons," *Rev. Mod. Phys.*, **47**, 713–761 (1975).

3) B. L. Berman *et al.*, "Absolute photoneutron cross sections for Zr, I, Pr, Au and Pb," *Phys. Rev. C*, **36**, 1286–1292 (1987).
4) V. V. Varlamov, N. N. Peskov *et al.*, *Consistent Evaluation of Photoneutron Reaction Cross Sections Using Data Obtained in Experiments with Quasimonoenergetic Annihilation Photon Beams at Livermore (USA) and Saclay (France)*, INDC (CCP)-440, IAEA, Issue 1–2 (2003).
5) T. S. Park, J. M. Lee, H. Y. Hwang, "Standardization of ^{152}Eu and ^{88}Y," *Appl. Radiat. Isot.*, **56**, 275–280 (2002).
6) YU. Khazov, A. A. Rodionov, S. Sakharov, B. Singh, *Chart of Nuclide*, NNDC, http://www.nndc.bnl.gov/chart/.
7) B. Singh, "Nuclear data sheets for $A = 89$," *Nuclear Data Sheets*, **85**, 1–170 (1998).
8) A. Veyssiere *et al.*, "Photoneutron cross sections of ^{208}Pb and ^{197}Au," *Nucl. Phys. A*, **159**, 561–576 (1970).
9) S. C. Fultz *et al.*, "Photoneutron cross section measurement on gold using nearly monoenergetic photons," *Phys. Rev.*, **127**, 1273–1279 (1962).
10) V. V. Varlamov *et al.*, "Photoneutron reaction cross sections in experiments with beams of quasimonoenergetic annihilation photons," *J., YK.*, **1–2**, 48 (2003), [in Russian].
11) K. Vogt *et al.*, "Measurement of the (γ, n) cross section of the nucleus ^{197}Au close above the reaction threshold," *Nucl. Phys. A*, **707**, 241–252 (2002).
12) K. Y. Hara *et al.*, "Measurement of the ^{152}Sm(γ, n) cross section with laser-Compton scattering gamma rays and the photon difference method," *J. Nucl. Sci. Technol.*, **44**[7], 938–945 (2007).
13) Y. Han, Y.-O. Lee, *High Energy Photonuclear Library*, NDEL, KAERI (1999).
14) B. L. Berman, J. T. Caldwell *et al.*, "Photoneutron cross sections for Zr^{90}, Zr^{91}, Zr^{92}, Zr^{94} and Y^{89}," *Phys. Rev.*, **162**[4], 1098–1111 (1967).
15) B. L. Berman, R. L. Bramblett *et al.*, "Photoneutron cross sections for As^{75}, Ag^{107} and Cs^{133}," *Phys. Rev.*, **177**[4], 1745–1754 (1969).
16) A. Lepretre, H. Beil *et al.*, "The giant dipole states in the A = 90 mass region," *Nucl. Phys. A*, **175**, 609–628 (1971).
17) A. Lepretre, H. Beil, R. Bergere, P. Carlos, A. Deminiac, A. Veyssiere, "A study of the giant dipole resonance of vibrational nuclei in the A = 103–133 mass region," *Nucl. Phys. A*, **219**, 39–60 (1974).
18) C. M. Baglin, "Nuclear data sheets for $A = 92$," *Nuclear Data Sheets*, **91**, 423–584 (2000).
19) *Atlas of GDR Parameters*, IAEA-TECDOC-1178, IAEA (2000).
20) H. Beil *et al.*, "A study of the photoneutron contribution to the giant dipole resonance in doubly even Mo isotopes," *Nucl. Phys. A*, **227**, 427–449 (1974).